Pulmonary Administration of a Water-Soluble Curcumin Complex Reduces Severity of Acute Lung Injury

Madathilparambil V. Suresh[1], Matthew C. Wagner[4], Gus R. Rosania[2], Kathleen A. Stringer[3], Kyoung Ah Min[2], Linda Risler[5], Danny D. Shen[5], George E. Georges[5], Aravind T. Reddy[4], Jaakko Parkkinen[5,6], and Raju C. Reddy[4]

[1]Department of Surgery, [2]Department of Pharmaceutical Sciences, College of Pharmacy, and [3]Department of Clinical, Social, and Administrative Sciences, College of Pharmacy, University of Michigan, Ann Arbor, Michigan; [4]Division of Pulmonary, Allergy, and Critical Care Medicine, Department of Medicine, Emory University and Atlanta Veterans Affairs Medical Center, Atlanta, Georgia; [5]Fred Hutchinson Cancer Research Center, Seattle, Washington; and [6]Institute of Biomedicine, University of Helsinki, Helsinki, Finland

Local or systemic inflammation can result in acute lung injury (ALI), and is associated with capillary leakage, reduced lung compliance, and hypoxemia. Curcumin, a plant-derived polyphenolic compound, exhibits potent anti-inflammatory properties, but its poor solubility and limited oral bioavailability reduce its therapeutic potential. A novel curcumin formulation (CDC) was developed by complexing the compound with hydroxypropyl-γ-cyclodextrin (CD). This results in greatly enhanced water solubility and stability that facilitate direct pulmonary delivery. *In vitro* studies demonstrated that CDC increased curcumin's association with and transport across Calu-3 human airway epithelial cell monolayers, compared with uncomplexed curcumin solubilized using DMSO or ethanol. Importantly, Calu-3 cell monolayer integrity was preserved after CDC exposure, whereas it was disrupted by equivalent uncomplexed curcumin solutions. We then tested whether direct delivery of CDC to the lung would reduce severity of ALI in a murine model. Fluorescence microscopic examination revealed an association of curcumin with cells throughout the lung. The administration of CDC after LPS attenuated multiple markers of inflammation and injury, including pulmonary edema and neutrophils in bronchoalveolar lavage fluid and lung tissue. CDC also reduced oxidant stress in the lungs and activation of the proinflammatory transcription factor NF-κB. These results demonstrate the efficacy of CDC in a murine model of lung inflammation and injury, and support the feasibility of developing a lung-targeted, curcumin-based therapy for the treatment of patients with ALI.

Keywords: cyclodextrin; LPS; turmeric; Calu-3; oxidative stress; TEER

Acute lung injury (ALI) can result from a variety of pulmonary and extrapulmonary insults, and is characterized by capillary leakage with resultant pulmonary edema and hypoxemia (1). In the early acute phase, ALI exhibits severe neutrophil-rich alveolar inflammation (2) and associated oxidant stress (3). The result is epithelial and endothelial injury that increases permeability and impairs fluid clearance. Mortality remains high, and no effective pharmacotherapy exists (4). Novel therapies for ALI are therefore urgently needed.

Curcumin, a polyphenolic compound from the rhizome of the *Curcuma longa* plant commonly known as turmeric, has been shown to exhibit a number of beneficial effects (5) that are exerted through a wide variety of signaling pathways (6–9). These effects include potent anti-inflammatory and antioxidant activities. Although the use of curcumin appears potentially attractive in a number of disease states, clinical applications have been restricted because its limited water solubility and oral bioavailability make it difficult to achieve therapeutically useful concentrations. For example, Garcea and colleagues found plasma concentrations only in the low nanomolar range after oral doses of 450–3,600 mg/day for 1 week (10). Others have similarly observed very low or undetectable plasma concentrations after doses up to 8 g/day or 12 g as a single dose (11, 12). The oral bioavailability of curcumin is similarly limited in the mouse, with plasma concentrations in the low nanomolar range after daily doses of 300 mg/kg by oral gavage (13).

We recently developed a stable, water-soluble formulation of curcumin (CDC) in which the compound is complexed with hydroxyalkyl-substituted γ-cyclodextrin (CD) (14). This formulation can be administered in ways not feasible with free curcumin, including delivery directly to the lung. Direct pulmonary administration is particularly attractive for lung diseases such as ALI because it bypasses the systemic circulation, thus reducing the potential for both metabolic breakdown and unwanted systemic effects. This route of administration also directly targets the drug to the site of therapeutic action. Direct pulmonary delivery is further supported by the canine pharmacokinetic study reported here, which demonstrates rapid plasma elimination of curcumin after intravenous CDC administration. However, it is possible that the complexation of curcumin with cyclodextrins may alter the activity of the compound and impair cell penetration. We therefore tested the ability of CDC to penetrate and permeate human airway-derived epithelial cells, and determined whether intratracheally instilled CDC reduced inflammation and injury in a murine model of ALI induced by LPS.

MATERIALS AND METHODS

Cell Culture

Cell culture methods are described in the online supplement.

Curcumin Transport across the Calu-3 Cell Monolayer

A more detailed description of these methods is provided in the online supplement.

Evaluation of Cell-Associated Curcumin

Methods for the qualitative and quantitative determination of curcumin concentrations associated with Calu-3 cells are described in the online supplement. Cell-associated curcumin was detected with the FITC channel of an epifluorescence microscope, as previously described (15–17).

(*Received in original form May 27, 2011 and in final form January 27, 2012*)

This work was supported by National Institutes of Health grants AI079539 (R.C.R.), HL093196 (R.C.R.), and GM078200 (G.R.R.).

Correspondence and requests for reprints should be addressed to Raju C. Reddy, M.D., Division of Pulmonary, Allergy, and Critical Care Medicine, Department of Medicine, Emory University/Atlanta Veterans Affairs Medical Center, 1670 Clairmont Road, Atlanta, GA 30033. E-mail: raju.reddy@emory.edu

This article has an online supplement, which is accessible from this issue's table of contents at www.atsjournals.org

Am J Respir Cell Mol Biol Vol 47, Iss. 3, pp 280–287, Sep 2012
Published 2012 by the American Thoracic Society
Originally Published in Press as DOI: 10.1165/rcmb.2011-0175OC on February 3, 2012
Internet address: www.atsjournals.org

Animals

Male C57BL/6 mice at 6 to 8 weeks of age were obtained from Jackson Laboratories (Bar Harbor, ME). Beagles were purchased from commercial kennels and raised at the Fred Hutchinson Cancer Research Center (FHCRC). All experimental animal care and treatments followed guidelines established by the University of Michigan, the Atlanta Veterans Affairs Medical Center, and the FHCRC Committees on the Use and Care of Animals.

LPS and Curcumin Administration

Mice were anesthetized with 50 mg/kg ketamine and 5 mg/kg xylazine, administered via intraperitoneal injection. A tracheotomy was performed, and mice were injected intratracheally with 50 μg/50 μl of *Escherichia coli* LPS O111:B4 (Sigma-Aldrich, St. Louis, MO) or vehicle (PBS). Two hours later, they received 30 μg/50 μl of curcumin as CDC or vehicle (CD).

Bronchoalveolar Lavage Fluid Protein and Cell Count

Bronchoalveolar lavage (BAL) fluid was collected by flushing 3 × 1 ml of PBS into the lung via a tracheal cannula. The BAL fluid was centrifuged at 500 × *g* at 4°C for 5 minutes. The supernatant was analyzed for total protein, using the BCA Protein Assay Kit (Pierce, Rockford, IL). Pelleted cells were then resuspended in 1 ml of PBS. Total cell number was counted by hemocytometer, and a differential cell count was performed by cytospin staining with Diff-Quik (Scientific Products, McGaw Park, IL).

Nuclear Protein Preparation and NF-κB Transcription Factor Assay

Nuclear protein from lung tissue was isolated using a nuclear protein extraction kit (Cayman Chemical, Ann Arbor, MI). NF-κB activity was measured using the ELISA-based NF-κB (p65) Transcription Factor Assay Kit (Cayman Chemical).

Wet/Dry Weight Ratio and Lung Histology

These methods are described in the online supplement.

Measurement of Oxidant Stress

The production of H_2O_2 in lung tissue was determined using the Amplex Red Hydrogen Peroxide Assay Kit (Molecular Probes, Eugene, OR) according to the manufacturer's instructions. The fluorescence intensity of samples and standards was measured in a plate reader (Perkin-Elmer, Waltham, MA) with excitation (EX) at 560 nm and emission (EM) at 590 nm. The concentrations of nitrate and malondialdehyde in lung homogenates were measured using commercially available colorimetric assay kits (Cayman Chemical), according to the manufacturer's instructions.

Statistical Analysis

Data are presented as means ± SD. For the sample analyses, the Tukey multiple comparison test was applied after ANOVA, using GraphPad Prism version 5.03 (GraphPad Software, La Jolla, CA). $P < 0.05$ was considered statistically significant.

RESULTS

Curcumin Association with and Transport by Human Lung Epithelial Cells

The local absorption, tissue distribution, and intracellular accumulation of drug molecules can be a critical determinant of drug efficacy. The epithelial lining of the lung serves as a barrier preventing the absorption of inhaled substances, thus potentially blocking the ability of inhaled drugs to reach the underlying endothelial cells and interstitial spaces where inflammatory cells can accumulate. The ability of epithelial cells to take up and transport curcumin *in vitro* was therefore used to assess whether the CDC formulation may be adequate as an ALI treatment. For this purpose, we used a standard human lung epithelial cell line, Calu-3 cells, grown in an air–liquid interface system that resembles the natural conditions in the lungs (18). Both the apical-to-basolateral (AP→BL) and basolateral-to-apical (BL→AP) transports of CDC solutions in Hanks' balanced salt solution transport buffer were examined over a range of therapeutically relevant concentrations (0–200 μM). For comparison, we performed similar studies using a standard, commercially available curcumin diluted from stock solutions prepared in DMSO (DMSO-C) or ethanol (EtOH-C). We found that 200-μM concentrations of CDC produced curcumin transport rates across intact cell monolayers at rates as high as 22×10^{-5} nmol per second. At an equivalent curcumin concentration, DMSO-C or EtOH-C showed slightly higher mass transport rates (Figure 1A), but cell monolayers were disrupted. The observed curcumin mass transport rates were concentration-dependent and were higher in the AP→BL than in the BL→AP transport direction.

The cellular permeability coefficient (P_{eff}), a parameter describing the mass transport rate normalized by the donor initial concentration and monolayer area, for the AP→BL direction was maximal at 50 μM, and appeared to decrease with increasing curcumin concentrations in the donor compartment, suggesting a complex transport pathway (Figure 1B, *top*). P_{eff} in the BL→AP direction was much lower than in the AP→BL direction (Figure 1B, *bottom*), consistent with a cellular mechanism selectively facilitating the passage of curcumin in the AP→BL direction. P_{eff} in the BL→AP direction was relatively constant at different donor drug concentrations, with no evidence of saturation. The P_{eff} for CDC was greater than that for either DMSO-C or EtOH-C at 50 μM in the AP→BL direction, and at both concentrations in the BL→AP direction.

In all studies, Lucifer Yellow (LY) transport was also measured. As a hydrophilic, membrane-impermeant compound (MW 457), LY is commonly used as a marker for paracellular transport (19). The calculated P_{eff} of LY was very low ($P_{eff,\ \text{AP}\rightarrow\text{BL}}$, $8.21 \times 10^{-8} \pm 2.99 \times 10^{-8}$ cm/s; $P_{eff,\ \text{BL}\rightarrow\text{AP}}$, $4.69 \times 10^{-8} \pm 2.72 \times 10^{-8}$ cm/s), thus confirming the integrity of the cellular monolayers for the transport experiments. In addition, monolayer integrity before and after transport studies was independently established by the measurement of transepithelial electrical resistance (TEER). TEER values were unchanged in 50 μM CDC in the AP→BL direction, and in 50 μM and 100 μM CDC in the BL→AP direction, although TEER decreased slightly with increasing curcumin concentrations. The 200-μM (donor) concentrations of DMSO-C and EtOH-C decreased TEER values from $422 \pm 6\ \Omega \cdot \text{cm}^2$ to $176 \pm 12\ \Omega \cdot \text{cm}^2$, and from $418 \pm 3\ \Omega \cdot \text{cm}^2$ to $152 \pm 9\ \Omega \cdot \text{cm}^2$, respectively, in the AP→BL direction, suggesting the disruption of monolayer integrity. In 200 μM CDC, TEER values changed from $423 \pm 5\ \Omega \cdot \text{cm}^2$ to $351 \pm 13\ \Omega \cdot \text{cm}^2$. Nevertheless, TEER values remained greater than $350\ \Omega \cdot \text{cm}^2$, consistent with the preservation of monolayer integrity.

We next assessed the extent to which Calu-3 cells accumulated curcumin in the CD solutions. First, inserts were examined with the ×10 objective of a fluorescence microscope, after incubation with the nucleus-specific molecular probe Hoechst 33342 (10 μg/ml). Cell-associated curcumin was detected in the FITC channel, and nuclei were visualized in the DAPI channel. Microscopic examination indicated the concentration-dependent cell association of curcumin, which was greater after exposure on the apical side than on the basolateral side (Figure 2A). Our methods cannot determine whether this cell association represents extracellular attachment or intracellular uptake, although we found it was not removed by rinsing.

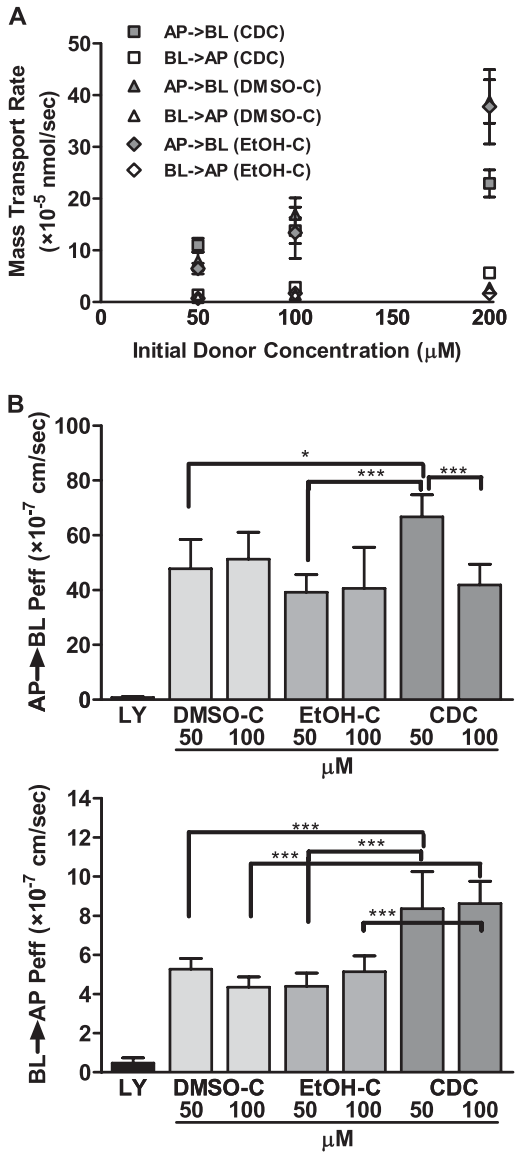

Figure 1. A stable, water-soluble formulation of curcumin (CDC), in which the compound is complexed with hydroxyalkyl-substituted γ-cyclodextrin (CD), promotes curcumin transport across lung epithelial cells. Calu-3 cell monolayers were grown on Transwell inserts. CDC, commercially available curcumin diluted from stock solutions prepared in DMSO (DMSO-C), commercially available curcumin diluted from stock solutions prepared in ethanol (EtOH-C), or Lucifer Yellow (LY) was added to Hanks' balanced salt solution (HBSS) transport buffer in either the apical (AP) or basolateral (BL) compartment. The contralateral compartment was sampled at intervals, and curcumin or LY concentrations were measured by fluorescence, using a plate reader set to 485 nm (excitation)/540 nm (emission). (*A*) Mass transport rate as a function of the initial donor concentration of CDC, DMSO-C, or EtOH-C for the AP→BL and BL→AP directions. (*B*) The cellular permeability coefficient (P_{eff}) for the AP→BL (*top*) or BL→AP (*bottom*) directions of LY (paracellular marker, 1 mM), DMSO-C, EtOH-C, and CDC as a function of initial donor concentration ($n = 6$). *$P < 0.05$. ***$P < 0.001$.

To quantify cell-associated curcumin, additional Calu-3 cell monolayers on inserts were incubated for 90 minutes with 1% Triton X-100, and the mass of curcumin extracted from the cell monolayers was measured. This value was normalized by the number of cells on the membranes (detached by trypsinization), and plotted as cell-associated mass per cell (Figures 2B and 2C). The cell-associated curcumin mass increased in proportion to the extracellular curcumin concentration under all conditions examined (Figure 2B). A significantly greater curcumin mass was observed after apical exposure to CDC than to DMSO-C or EtOH-C, but the curcumin mass associated with cells from the basolateral compartment was similar under all conditions tested (Figures 2B and 2C).

Because the absorption of inhaled drug formulations involves a transient drug exposure, the tightness of cell-to-cell contacts as measured by the TEER value is a key, highly sensitive indicator of epithelial barrier function. Because exposure to DMSO-C or EtOH-C concentrations greater than or equal to 100 μM led to significant changes in TEER values after transport, we used microscopy to assess the effects of CDC, DMSO-C, and EtOH-C on cell monolayer integrity over the course of the transport studies. Following CDC exposure, microscopic analysis revealed no evidence of cell–cell separation or detachment under any condition (Figure 2A). With DMSO-C or EtOH-C, however, evidence of cell rounding and cell–cell disruption appeared at 100 μM, and was prominent at the 200-μM concentration for AP→BL transport. Cell monolayer integrity was compromised at 200 μM for BL→AP transport, whether the initial solvent was DMSO or ethanol (Figure 2A).

Pharmacokinetics and Toxicology after Systemic CDC Administration

CDC was administered intravenously to beagles at doses as high as 10 mg/kg twice daily for 14 days, with no adverse effects being observed in any dog (online supplement). The pharmacokinetics of curcumin was also assessed. Both curcumin and its principle metabolite, tetrahydrocurcumin, disappeared rapidly, and plasma concentrations were undetectable after 30 minutes. After repeated daily administration, tetrahydrocurcumin sulfate became a major metabolite, peaking at 30 minutes and largely disappearing by 60 minutes. This rapid plasma clearance of curcumin after systemic CDC administration supports our choice of pulmonary administration for further *in vivo* studies.

Curcumin Deposition in the Lungs

To test the efficacy of pulmonary CDC delivery in a relevant animal model of ALI, we extended our *in vitro* studies by first determining the extent of curcumin accumulation on or in lung cells after an intratracheal administration of CDC. One hour after the intratracheal administration of CDC (Figure 3, *bottom*) or vehicle (Figure 3, *top*) the lungs were removed, fixed, and sectioned. Sections were examined by light microscopy and by fluorescence microscopy at curcumin-specific excitation and detection wavelengths. Some intrinsic autofluorescence was observed at these wavelengths, but fluorescence was much brighter after curcumin administration, and was prominent throughout most of the lung. These observations support successful delivery to cellular targets in this organ.

Inhibition of LPS-Induced Lung Inflammation and Injury by CDC Administration

Because our data demonstrated that the potent anti-inflammatory agent curcumin is extensively taken up by cells throughout the lung after CDC administration, we tested whether CDC could inhibit the lung inflammation induced by LPS in a well-characterized murine model of ALI. LPS was administered intratracheally to mice, followed by CDC (30 μg) or vehicle 2 hours later. The dose of CDC was based on preliminary dose–response studies (data not shown). Four hours after the CDC dose, BAL fluid was collected,

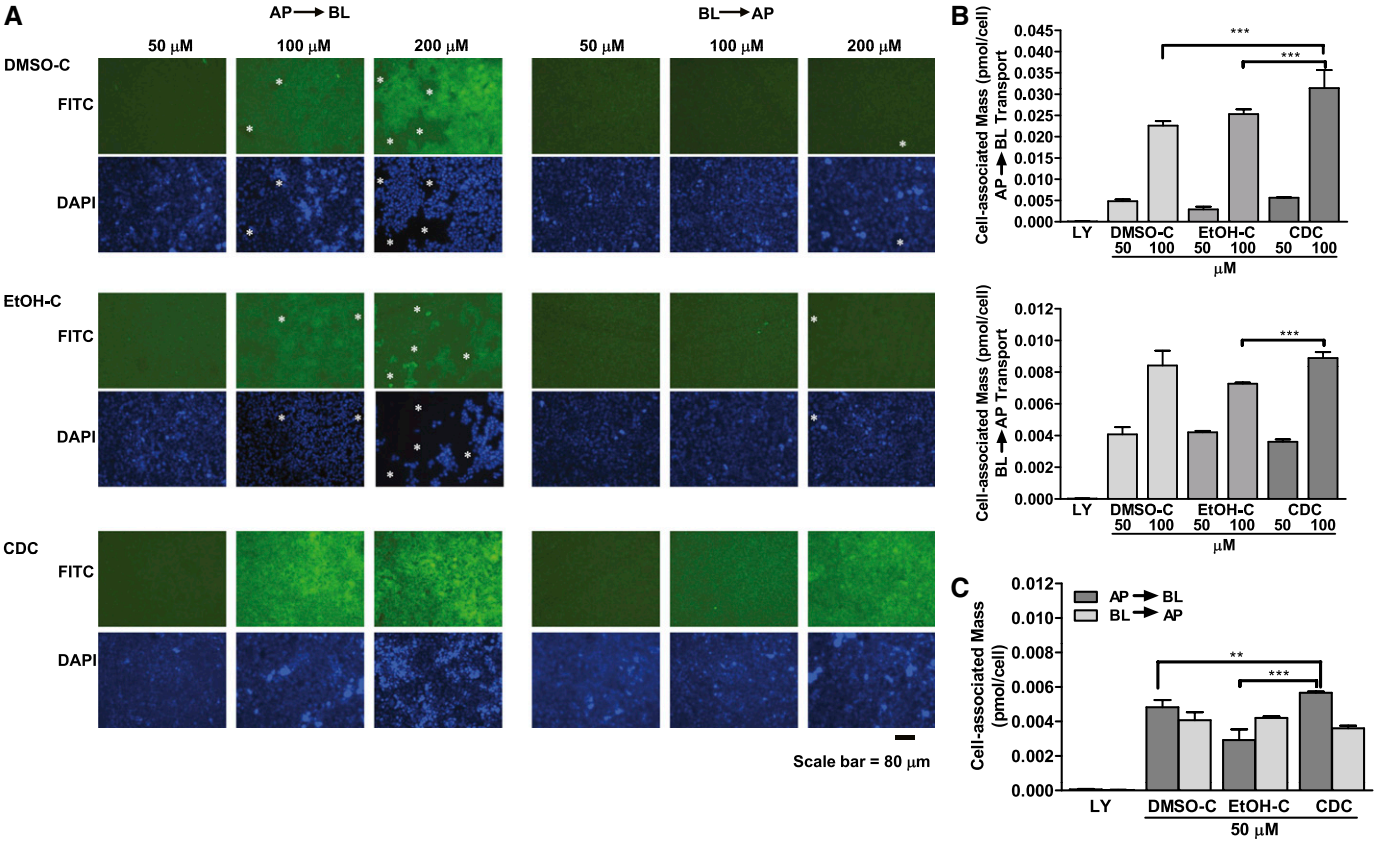

Figure 2. CDC promotes the association of curcumin with lung epithelial cells. Calu-3 cell monolayers on Transwell inserts were exposed to CDC, DMSO-C, or EtOH-C in either the apical (AP→BL) or basolateral (BL→AP) compartments for 180 minutes, with shaking at 37°C in a 5% CO_2 incubator. (*A*) The inserts were then washed and incubated for another 30 minutes with the nucleus-specific dye Hoechst 33342 (10 μg/ml) in the apical compartment, and with dye-free HBSS transport buffer in the basolateral compartment. Cell monolayers were examined with a Nikon TE 2000 fluorescence microscope (×10 objective) (Nikon Instruments, Melville, NY). Curcumin was visualized in the FITC channel, and nuclei were visualized in the DAPI channel. Regions where cells have detached or where monolayer integrity is visibly compromised are indicated with an asterisk. *Scale bar* of 80 μm is displayed. Representative images are shown from three independent experiments. (*B* and *C*) After exposure, cells were washed, and cell-associated curcumin was extracted with 1% Triton X-100. Extracted curcumin was quantitated (mass per cell) by fluorescence, using a plate reader. Amounts of the paracellular marker LY are also shown. (*B*) Cell-associated curcumin as a function of the initial donor concentration for AP→BL (*top*) and BL→AP (*bottom*) transport. (*C*) Cell-associated curcumin as a function of transport direction at 50 μM ($n = 6$). $^{**}P < 0.01$. $^{***}P < 0.001$.

and the lungs were prepared for the microscopic examination of lung injury. Both cell counts (Figure 4A, *left*) and microscopy (Figure 4B) showed notably fewer cells in BAL fluid from CDC-treated than from vehicle-treated mice. Furthermore, whereas a majority of cells in the BAL fluid of vehicle-treated mice comprised inflammation-related neutrophils, this proportion was markedly reduced after CDC treatment (Figure 4A, *right*).

The activation of specific transcription factors, notably NF-κB, and the consequent production of proinflammatory cytokines and other molecules comprise prominent features of inflammation. We next tested whether reduced inflammation is reflected in the down-regulation of NF-κB activity. Nuclear protein was isolated from the lungs of mice treated with LPS and CDC or vehicle, and NF-κB activity was determined. The increase in activity after LPS treatment was significantly reduced by CDC (Figure 4C). Inflammation and the activation of NF-κB up-regulated the production of reactive oxygen species, and thus oxidant stress. Measured markers of LPS-induced oxidant stress (i.e., H_2O_2 production, nitrate concentration, and malonaldehyde as a measure of lipid peroxidation) were also attenuated by CDC treatment (Figure 4C).

To assess further the ability of CDC to inhibit LPS-induced lung injury, we measured the amount of protein in BAL fluid. Protein was significantly increased by LPS, but this increase was largely blocked by CDC treatment (Figure 5A). We also examined changes in the ratio of wet/dry weight in lung tissue, a quantitative measure of vascular permeability and resultant edema (20). We found that LPS treatment produced significant increases in the wet/dry weight ratio, and CDC attenuated this increase (Figure 5A). A histopathological examination of hematoxylin and eosin–stained lung tissue also showed reductions in inflammatory markers after CDC treatment (Figure 5B).

DISCUSSION

The clinical use of curcumin has been limited by its low solubility and poor oral bioavailability. Delivery by inhalation for the treatment of pulmonary disease likewise appears infeasible, because the organic solvents in which it must be dissolved are toxic to the lung. To overcome these drug-delivery obstacles, we developed a new formulation of curcumin in which it is complexed with hydroxypropyl ether derivatives of cyclodextrin (CD). This formulation of curcumin is stable, highly water-soluble, bioavailable, and easily produced (14, 21, 22). This permits administration by either the intravenous or inhalation routes at doses that have been shown to elicit anti-inflammatory effects. However, preliminary studies in beagles (online supplement) showed that

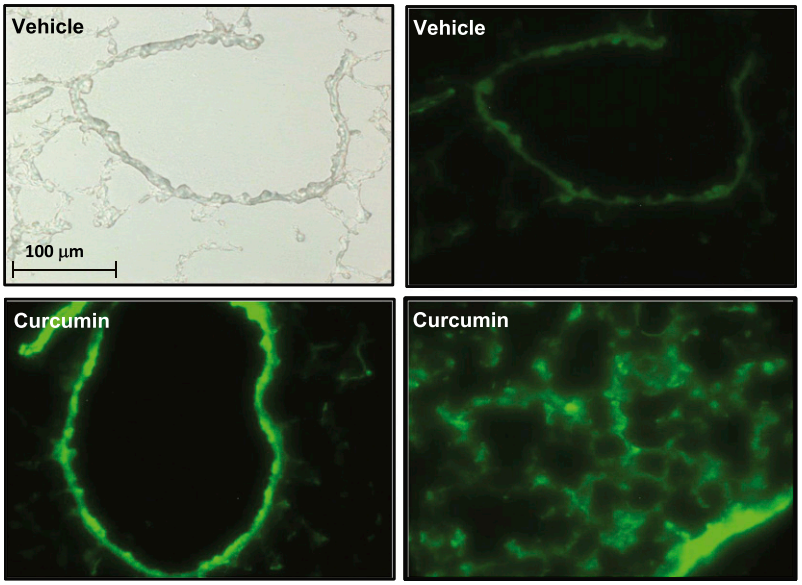

Figure 3. CDC fluorescence is associated with lung cells *in vivo*. C57BL/6 mice received CDC (30 μg) or vehicle intratracheally. One hour later, the lungs were embedded in optimal cutting temperature compound, frozen, and sectioned. Sections were examined by light microscopy (*top left*) or fluorescence microscopy, with curcumin visualized in the FITC channel. *Bottom right*: Lung parenchyma. Other images represent cross sections of airways. Representative images are shown from three independent experiments.

CDC is rapidly cleared from the circulation after intravenous administration. Furthermore, the oral bioavailability of curcumin is low because of metabolism in the intestine (23), which would presumably affect oral CDC as well. These limitations make inhalation a viable route of administration for CDC, particularly for the targeted treatment of inflammatory lung disease.

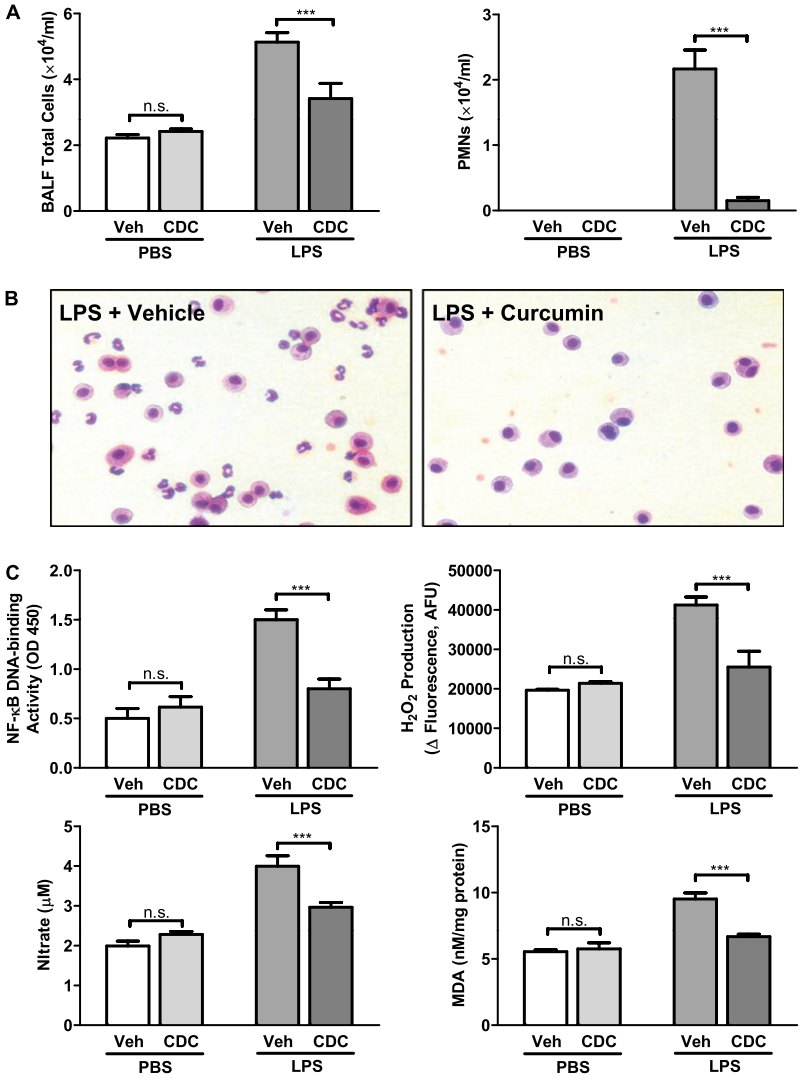

Figure 4. CDC reduces LPS-induced lung inflammation. ALI was induced by an intratracheal administration of LPS (50 μg). CDC (30 μg) or vehicle (CD) was administered 2 hours later. Bronchoalveolar lavage fluid (BALF) was collected, and lungs were excised after 4 hours. (*A*) BALF was centrifuged at 500 × *g* for 5 minutes. Pelleted cells were washed, and the cellular content of the resuspended pellet was determined via cytospin. (*B*) Cells from BALF were stained with Diff-Quik and examined microscopically. (C) Nuclear protein was isolated from lungs, and NF-κB activity was determined using an ELISA-based assay kit (*top left*). Lung tissue was homogenized, and oxidant stress was assessed by measuring H_2O_2 production (*top right*), nitrate (*bottom left*), and malonaldehyde (MDA; *bottom right*), using commercially available kits ($n = 16$–18 mice/group). ***$P <$ 0.001. n.s., not significant; PMNs, polymorphonuclear leukocytes; Veh, vehicle.

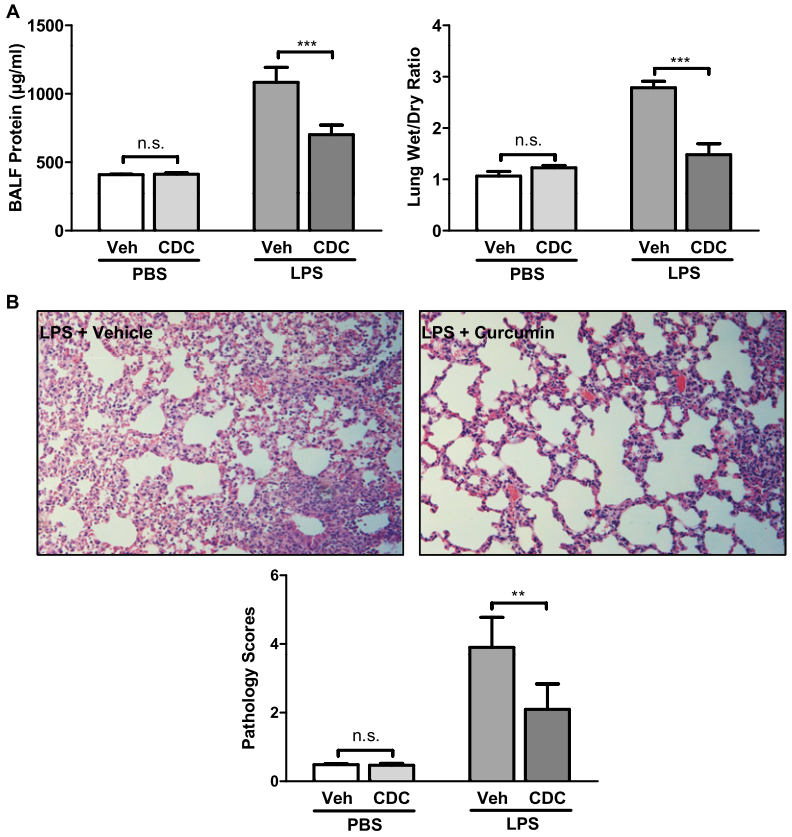

Figure 5. CDC attenuates lung injury and edema after LPS administration. ALI was induced by intratracheal administration of LPS (50 μg). CDC (30 μg) or vehicle (CD) was administered 2 hours later, and BALF was collected after 4 hours. (*A*) *Left*: Cells in BALF were pelleted by centrifugation, after which the protein content of the supernatant was determined as a marker of lung injury. Before BALF was collected, the superior lobe of the left lung was excised and immediately weighed. It was then dried in an incubator at 60°C for 24 hours and weighed again. *Right*: The ratio of wet/dry weight was determined as an index of edema. (*B*) *Top*: Lungs were fixed, sectioned, and stained with hematoxylin and eosin. Representative sections were then examined microscopically. *Bottom*: The degree of injury (Pathology Scores) was calculated according to the scale: 1, no injury; 2, injury to 25% of the field; 3, injury to 50% of the field; 4, injury to 75% of the field; and 5, diffuse injury (n = 16–18 mice/group). $^{**}P < 0.01$. $^{***}P < 0.001$.

In this study, we delivered intratracheal CDC to ensure that the dose was delivered to the lungs. The pulmonary delivery of a nebulized preparation via the oropharyngeal cavity may be more directly relevant to human use, but in rodents (obligate nose breathers) most of the drug is deposited in the nasal passages and upper respiratory tract (24). Therefore, intratracheal administration is the preferred method for proof-of-concept studies in which accurate dosage is required.

One major advantage of the CDC formulation involves its ease of preparation. Curcumin is dissolved at high pH, hydroxypropyl-γ-cyclodextrin is added at a slight molar excess, and after a brief period of agitation, the solution is neutralized. Previous attempts to solubilize curcumin with cyclodextrin or its derivatives did not use elevated pH (21). These formulations required large molar excesses of cyclodextrin, and achieved much lower concentrations of solubilized curcumin. As previously reported (14), the CDC formulation is also much more stable in solution than were those formulations. A wide variety of other methods have been used to improve curcumin solubility. These include microemulsions, nanoemulsions, liposomes, several types of encapsulated nanoparticles, and self-microemulsifying drug-delivery systems, as well as surfactants and solvents (22). Many of these formulations have exhibited a degree of success in preclinical studies (25). However, all of these approaches involve more complex procedures than those used to prepare CDC, and many produce smaller incremental improvements in curcumin solubility (22). Furthermore, because these formulations were developed for intravenous use or with the goal of improving oral bioavailability, their suitability for pulmonary delivery remains unclear.

Our present experiments show that curcumin transport is promoted by CDC in lung epithelial cells *in vitro* and by lung tissues *in vivo*. The Calu-3 cell line constitutes a well-established cell model for the quantitative evaluation of mechanisms and pharmacokinetics (e.g., drug absorption or toxicity) of formulations of lung-targeted or inhaled molecules, and has been used to characterize *in vitro–in vivo* associations for various drug molecules (26–29). Our findings of increased curcumin association with Calu-3 cells agree with previous reports indicating that CD formulations promote the uptake of highly insoluble drugs in other *in vitro* cell models (14). Cyclodextrins were previously tested in nebulized, inhaled drug formulations, with some reports indicating that CDs enhance pulmonary penetration (30–32). For these experiments, Calu-3 cell monolayers were used as a standard reference cell line for establishing the transport properties of drug formulations (32–34). However, previous reports indicated that CDs promoted delivery, not by directly enhancing permeability or cell association, but by acting as a reservoir for the drug and promoting its dispersion (35–37). Because CDs are cell-impermeant (30, 35, 36), curcumin–CD complexes may plausibly inhibit the intracellular uptake of curcumin. Nevertheless, our *in vitro* and *in vivo* experiments demonstrated that CD increased the amount of delivered and cell-associated curcumin and its transcellular permeability, with an associated enhancement of efficacy in experimental ALI.

The CD-enhanced delivery of curcumin to lung cells, together with the well-known anti-inflammatory and antioxidant effects of curcumin (5), led us to test the ability of CDC to reduce inflammation in a murine model of ALI. ALI is associated with the influx of inflammatory cells, especially neutrophils, into the lungs, and we found that CDC administration after the induction of ALI significantly reduced both total cell and neutrophil counts. In addition, CDC down-regulated the activity of the proinflammatory transcription factor NF-κB and reduced oxidant stress. These findings provide *in vivo* confirmation of previous *in vitro* observations that CDC reduced NF-κB activity more effectively than uncomplexed curcumin (14). In other settings, curcumin was shown to down-regulate the activity of not

only NF-κB but also the proinflammatory transcription factors AP-1 (38) and HIF-1α (39). The production of proinflammatory cytokines, and thus subsequent inflammatory changes, are largely dependent on the activation of these transcription factors, and therefore the decreased NF-κB activity provides a molecular mechanism for the observed decrease in inflammatory markers.

To our knowledge, there has been no previous demonstration that any curcumin formulation can effectively treat established ALI, although several previous studies showed that curcumin can at least partly prevent ALI when administered before the triggering event. In an LPS-induced model of ALI, Lian and colleagues found that intravenous curcumin dissolved in DMSO administered to rats 30 minutes before LPS reduced ALI severity (40). Olszanecki and colleagues administered curcumin intraperitoneally 2 hours before intraperitoneal LPS (41). They found that curcumin pretreatment decreased the sequestration of leukocytes by the lungs, and presented evidence that this decrease was mediated by the induction of heme oxygenase–1. We also found that the administration of intraperitoneal, but not oral, curcumin reduced the severity of inflammation after bleomycin-induced lung injury (13).

In Calu-3 cells, we observed that epithelial cell monolayer integrity was intact after transient exposures to CDC concentrations up to 200 μM, although monolayer integrity was visibly disrupted with lower doses of DMSO-C or EtOH-C. Given that the epithelial cell barrier is dependent on monolayer integrity, CDC appears to be safer than the DMSO or ethanol solutions commonly used to solubilize curcumin. Perhaps most importantly, preliminary toxicological studies of CDC in dogs similarly provided no evidence of adverse effects after doses up to 20 mg/kg/day for 14 days (online supplement).

Ours appears to be the first study of any curcumin formulation administered directly to the pulmonary system. Although we did not systematically investigate the toxicology of intratracheally delivered CDC, no drug-attributable toxicity was apparent in physiological parameters or on histopathological examination, even when the CDC concentration was increased to 600 μg (data not shown). Human studies of curcumin have revealed no adverse effects other than diarrhea after very high oral doses (12). By contrast, adverse effects are frequent with commonly used systemic anti-inflammatory agents. In ALI and acute respiratory distress syndrome (ARDS), results with systemic anti-inflammatory agents have been disappointing. Methylprednisolone in ARDS (42), as well as ketoconazole (43) and lisofylline (44) in mixed ALI/ARDS patient populations, have all proven ineffective. This ineffectiveness may reflect the adverse effects of these drugs, including interference with wound-healing. Significantly, dysfunctional wound-healing is thought to be a major pathophysiological factor in late-stage ARDS, and methylprednisolone appears to decrease survival when initiated more than 14 days after disease onset (42). Curcumin, by contrast, has been shown to promote wound-healing (5). Both the greater safety of CDC and its delivery directly to the target organ support the possibility that CDC may prove effective where other anti-inflammatory agents have not.

ALI remains a disease with high mortality and no effective treatment. Our results indicate that the direct delivery of CDC to the lungs is safe and effective in a murine model of ALI, and this effectiveness may be attributable to the association of CDC with the lung epithelium. The attractiveness of CDC is further increased by the ease and simplicity with which it can be produced. These promising early results support the potential of CDC as a possible therapy for human ALI and other inflammatory lung diseases.

Author disclosures are available with the text of this article at www.atsjournals.org.

References

1. Matuschak GM, Lechner AJ. Acute lung injury and the acute respiratory distress syndrome: pathophysiology and treatment. *Mo Med* 2010;107: 252–258.
2. Matute-Bello G, Frevert CW, Martin TR. Animal models of acute lung injury. *Am J Physiol Lung Cell Mol Physiol* 2008;295:L379–L399.
3. Ward PA. Oxidative stress: acute and progressive lung injury. *Ann N Y Acad Sci* 2010;1203:53–59.
4. Bosma KJ, Taneja R, Lewis JF. Pharmacotherapy for prevention and treatment of acute respiratory distress syndrome: current and experimental approaches. *Drugs* 2010;70:1255–1282.
5. Maheshwari RK, Singh AK, Gaddipati J, Srimal RC. Multiple biological activities of curcumin: a short review. *Life Sci* 2006;78:2081–2087.
6. Chen Y-R, Tan T-H. Inhibition of the c-Jun N-terminal kinase (JNK) signaling pathway by curcumin. *Oncogene* 1998;17:173–178.
7. Gaedeke J, Noble NA, Border WA. Curcumin blocks multiple sites of the TGF-β signaling cascade in renal cells. *Kidney Int* 2004;66:112–120.
8. Hu M, Du Q, Vancurova I, Lin X, Miller EJ, Simms HH, Wang P. Proapoptotic effect of curcumin on human neutrophils: activation of the p38 mitogen–activated protein kinase pathway. *Crit Care Med* 2005;33:2571–2578.
9. Zhou Y, Zheng S, Lin J, Zhang QJ, Chen A. The interruption of the PDGF and EGF signaling pathways by curcumin stimulates gene expression of PPARγ in rat activated hepatic stellate cell *in vitro*. *Lab Invest* 2007;87:488–498.
10. Garcea G, Jones DJ, Singh R, Dennison AR, Farmer PB, Sharma RA, Steward WP, Gescher AJ, Berry DP. Detection of curcumin and its metabolites in hepatic tissue and portal blood of patients following oral administration. *Br J Cancer* 2004;90:1011–1015.
11. Jurenka JS. Anti-inflammatory properties of curcumin, a major constituent of curcuma longa: a review of preclinical and clinical research. *Altern Med Rev* 2009;14:141–153.
12. Sharma RA, Gescher AJ, Steward WP. Curcumin: the story so far. *Eur J Cancer* 2005;41:1955–1968.
13. Smith MR, Gangireddy SR, Narala VR, Hogaboam CM, Standiford TJ, Christensen PJ, Kondapi AK, Reddy RC. Curcumin inhibits fibrosis-related effects in IPF fibroblasts and in mice following bleomycin-induced lung injury. *Am J Physiol Lung Cell Mol Physiol* 2010;298: L616–L625.
14. Yadav VR, Prasad S, Kannappan R, Ravindran J, Chaturvedi MM, Vaahtera L, Parkkinen J, Aggarwal BB. Cyclodextrin-complexed curcumin exhibits anti-inflammatory and antiproliferative activities superior to those of curcumin through higher cellular uptake. *Biochem Pharmacol* 2010;80:1021–1032.
15. Bisht S, Feldmann G, Soni S, Ravi R, Karikar C, Maitra A. Polymeric nanoparticle-encapsulated curcumin ("nanocurcumin"): a novel strategy for human cancer therapy. *J Nanobiotechnology* 2007;5:3.
16. Schiborr C, Eckert GP, Rimbach G, Frank J. A validated method for the quantification of curcumin in plasma and brain tissue by fast narrow-bore high-performance liquid chromatography with fluorescence detection. *Anal Bioanal Chem* 2010;397:1917–1925.
17. Mohorko N, Repovs G, Popovic M, Kovacs GG, Bresjanac M. Curcumin labeling of neuronal fibrillar tau inclusions in human brain samples. *J Neuropathol Exp Neurol* 2010;69:405–414.
18. Foster KA, Avery ML, Yazdanian M, Audus KL. Characterization of the Calu-3 cell line as a tool to screen pulmonary drug delivery. *Int J Pharm* 2000;208:1–11.
19. Lacombe O, Woodley J, Solleux C, Delbos JM, Boursier-Neyret C, Houin G. Localisation of drug permeability along the rat small intestine, using markers of the paracellular, transcellular and some transporter routes. *Eur J Pharm Sci* 2004;23:385–391.
20. Wang Y, Phelan SA, Manevich Y, Feinstein SI, Fisher AB. Transgenic mice overexpressing peroxiredoxin 6 show increased resistance to lung injury in hyperoxia. *Am J Respir Cell Mol Biol* 2006;34:481–486.
21. Tonnesen HH, Masson M, Loftsson T. Studies of curcumin and curcuminoids: XXVII. Cyclodextrin complexation: solubility, chemical and photochemical stability. *Int J Pharm* 2002;244:127–135.
22. Kumar A, Ahuja A, Ali J, Baboota S. Conundrum and therapeutic potential of curcumin in drug delivery. *Crit Rev Ther Drug Carrier Syst* 2010;27:279–312.
23. Shoba G, Joy D, Joseph T, Majeed M, Rajendran R, Srinivas PS. Influence of piperine on the pharmacokinetics of curcumin in animals and human volunteers. *Planta Med* 1998;64:353–356.

24. Southam DS, Dolovich M, O'Byrne PM, Inman MD. Distribution of intranasal instillations in mice: effects of volume, time, body position, and anesthesia. *Am J Physiol Lung Cell Mol Physiol* 2002;282:L833–L839.
25. Bisht S, Maitra A. Systemic delivery of curcumin: 21st century solutions for an ancient conundrum. *Curr Drug Discov Technol* 2009;6:192–199.
26. Forbes B. Human airway epithelial cell lines for *in vitro* drug transport and metabolism studies. *Pharm Sci Technol Today* 2000;3:18–27.
27. Mathia NR, Timoszyk J, Stetsko PI, Megill JR, Smith RL, Wall DA. Permeability characteristics of Calu-3 human bronchial epithelial cells: *in vitro–in vivo* correlation to predict lung absorption in rats. *J Drug Target* 2002;10:31–40.
28. Tronde A, Norden B, Marchner H, Wendel AK, Lennernas H, Bengtsson UH. Pulmonary absorption rate and bioavailability of drugs *in vivo* in rats: structure–absorption relationships and physicochemical profiling of inhaled drugs. *J Pharm Sci* 2003;92:1216–1233.
29. Ehrhardt C, Fiegel J, Fuchs S, Abu-Dahab R, Schaefer UF, Hanes J, Lehr CM. Drug absorption by the respiratory mucosa: cell culture models and particulate drug carriers. *J Aerosol Med* 2002;15:131–139.
30. Uekama K, Hirayama F, Irie T. Cyclodextrin drug carrier systems. *Chem Rev* 1998;98:2045–2076.
31. Loftsson T, Jarho P, Masson M, Jarvinen T. Cyclodextrins in drug delivery. *Expert Opin Drug Deliv* 2005;2:335–351.
32. Tewes F, Brillault J, Couet W, Olivier JC. Formulation of rifampicin–cyclodextrin complexes for lung nebulization. *J Control Release* 2008; 129:93–99.
33. Matilainen L, Toropainen T, Vihola H, Hirvonen J, Jarvinen T, Jarho P, Jarvinen K. *In vitro* toxicity and permeation of cyclodextrins in Calu-3 cells. *J Control Release* 2008;126:10–16.
34. Salem LB, Bosquillon C, Dailey LA, Delattre L, Martin GP, Evrard B, Forbes B. Sparing methylation of beta-cyclodextrin mitigates cytotoxicity and permeability induction in respiratory epithelial cell layers *in vitro*. *J Control Release* 2009;136:110–116.
35. Arima H, Yunomae K, Miyake K, Irie T, Hirayama F, Uekama K. Comparative studies of the enhancing effects of cyclodextrins on the solubility and oral bioavailability of tacrolimus in rats. *J Pharm Sci* 2001;90:690–701.
36. Davis ME, Brewster ME. Cyclodextrin-based pharmaceutics: past, present and future. *Nat Rev Drug Discov* 2004;3:1023–1035.
37. Nagarsenker MS, Meshram RN, Ramprakash G. Solid dispersion of hydroxypropyl beta-cyclodextrin and ketorolac: enhancement of *in-vitro* dissolution rates, improvement in anti-inflammatory activity and reduction in ulcerogenicity in rats. *J Pharm Pharmacol* 2000;52:949–956.
38. Huang TS, Lee SC, Lin JK. Suppression of c-Jun/AP-1 activation by an inhibitor of tumor promotion in mouse fibroblast cells. *Proc Natl Acad Sci USA* 1991;88:5292–5296.
39. Bae MK, Kim SH, Jeong JW, Lee YM, Kim HS, Kim SR, Yun I, Bae SK, Kim KW. Curcumin inhibits hypoxia-induced angiogenesis via down-regulation of HIF-1. *Oncol Rep* 2006;15:1557–1562.
40. Lian Q, Li X, Shang Y, Yao S, Ma L, Jin S. Protective effect of curcumin on endotoxin-induced acute lung injury in rats. *J Huazhong Univ Sci Technolog Med Sci* 2006;26:678–681.
41. Olszanecki R, Gebska A, Korbut R. The role of haem oxygenase-1 in the decrease of endothelial intercellular adhesion molecule–1 expression by curcumin. *Basic Clin Pharmacol Toxicol* 2007;101:411–415.
42. Steinberg KP, Hudson LD, Goodman RB, Hough CL, Lanken PN, Hyzy R, Thompson BT, Ancukiewicz M. Efficacy and safety of corticosteroids for persistent acute respiratory distress syndrome. *N Engl J Med* 2006;354:1671–1684.
43. ARDS Network. Ketoconazole for early treatment of acute lung injury and acute respiratory distress syndrome: a randomized controlled trial. The ARDS network. *JAMA* 2000;283:1995–2002.
44. ARDS Clinical Trials Network. Randomized, placebo-controlled trial of lisofylline for early treatment of acute lung injury and acute respiratory distress syndrome. *Crit Care Med* 2002;30:1–6.